

TiO₂ Nanotubes Promoted Pt-Ni/C Catalyst with Low Pt Content as Anode Catalyst for Direct Ethanol Fuel Cells

Lei Shen¹, Qi-Zhong Jiang^{1*}, Tao Gan¹, Min Shen², F.J. Rodriguez Varela³, A.L. Ocampo⁴ and Zi-Feng Ma¹

¹ Department of Chemical Engineering, Shanghai Jiao Tong University, Shanghai, China, 200240

² School of Chemical, Biological, and Materials Engineering, Sarkeys Energy Center, University of Oklahoma, Norman, U.S.A, 73019

³ Grupo de Recursos Naturales y Energéticos, Cinvestav Unidad Saltillo, Carr. Saltillo-Monterrey Km. 13, Ramos Arizpe, Coahuila, 25900, México

⁴ Facultad de Química, Departamento de Química Analítica, Universidad Nacional Autónoma de México, D.F. 04510, México, México

Received: November 20, 2009, Accepted: January 27, 2010

Abstract: TiO₂ nanotubes (TiO₂NTs) are added into a low-platinum content Pt-Ni/C catalyst to improve its catalytic activity for the ethanol oxidation reaction (EOR). The promotion effect of TiO₂NTs on Pt-Ni/C catalyst is studied. The results obtained by cyclic voltammetry (CV) and chronoamperometry indicate that TiO₂NTs can greatly enhance the catalytic activity of the Pt-Ni/C catalyst. Compared with a commercial Pt-Ru/C catalyst, the Pt-Ni-TiO₂NT/C catalyst has a larger electrochemical active surface (EAS) and shows lower onset potential for the EOR. The elemental composition and electronic structure of the catalyst are characterized by EDX, ICP-OES, XRD and XPS. Morphological properties of these catalysts are characterized by HRTEM. It can be concluded that the presence of TiO₂NTs can retain more of the Pt metallic species and provide more hydroxides groups, which results in a facile removal of reaction intermediates and lower onset oxidation potentials.

Keywords: DEFCs; Pt-Ni/C catalyst; TiO₂ nanotubes; Low Platinum; Anode catalyst

1. INTRODUCTION

Direct ethanol fuel cells (DEFCs) have attracted extensive research efforts, because ethanol is safer, more environmental friendly and has more energy density compared to methanol. Moreover, ethanol can be easily produced in large quantities from agricultural products [1-3]. Still, the commercialization of DEFCs has been hampered for several reasons, one of which is the fact that metallic Pt catalysts are readily poisoned by strongly adsorbed reaction intermediates such as CO_{ads} at low operating temperatures [1]. As in the case of the methanol oxidation, lots of work has been done to attempt to solve this problem. The most widely accepted strategy being the addition of a second transition metal [4-6] or a metal oxide component [7] to form a binary anode based on Pt. This Pt binary anode catalyst relies on the bi-functional mechanism [5] and the electronic ligand effect [8] to provide hydroxide groups which promote the removal of reaction intermediates by

oxidation [9] and weakening the intermediates absorption on the Pt sites [10, 11]. These two effects can improve the performance of DEFCs under operating conditions at temperatures near 80 °C.

So far, Pt-Ru/C alloys are considered as the best anode catalysts for the methanol oxidation reaction because of their tolerance to CO [12]. However, the performance of a Pt-Ru binary alloy is not the best for the EOR [13]. Furthermore, Pt and Ru are both noble metals. To decrease the cost of fuel cell catalysts, a cheap and readily scalable base metal for alloying with Pt is needed for DEFC anodes. Theoretical calculations have shown that Pt-Ni systems are more stable than other Pt alloys (e.g., Mo, Sn, etc.) [14]. Furthermore, in the potential range of the alcohol electro-oxidation process, Ni would not dissolve from the Pt-Ni system into the electrolyte, while Ru could dissolve from the alloy. The resistance to dissolution has been attributed to a passivated nickel hydroxide surface that enhances the stability of Ni in the Pt lattice [15]. Despite these apparent advantages, carbon supported Pt-Ni anodes have been only marginally studied [16]. In some cases, Ni has been introduced as the third element to improve the stability of

*To whom correspondence should be addressed: Email: qzjiang@sjtu.edu.cn

DEFC anode catalysts [17–19]. Z.B. Wang [17] and E. Ribadeneira [18] observed higher catalytic performances for the EOR and improved tolerance to CO of Pt–Ru–Ni/C anodes than Pt–Ru/C catalysts. Also, Spinacé et. al observed that Pt–Sn/C catalysts exhibited superior catalytic activity for the EOR when Ni was introduced as third element [19].

In this paper, we report the improvement in catalytic activity of Pt–Ni/C catalyst for the EOR by the introduction of a new oxide component. It has been shown that TiO₂ exhibits high catalytic activity for decomposition of small organic molecules [20]. Furthermore, TiO₂ has the additional advantage of being chemically stable even under acidic conditions [21]. TiO₂ has been reported as the support of Pt [22], Pd [23] or PtRu [24] catalysts, which have high catalytic activity and CO-tolerance during alcohol electro-oxidation reactions due to the interaction between the noble metals and the titanium oxide. It has been suggested that TiO₂ supports can modify the electronic structure of Pt [22], and provide additional oxygen sources of hydroxide or water molecules [25]. Moreover, our previous studies have shown that the introduction of TiO₂ nanotubes (TiO₂NTs) can greatly enhance the catalytic activities of Pt [25] or Pt–Ni [26] towards both CO and methanol electro-oxidation.

In the present study, we prepare the catalysts under continuous microwave irradiation which is distinct from the intermittent microwave condition we previously reported [26]. Here, the TiO₂NT functions as a catalyst promoter in the Pt–Ni–TiO₂/C catalyst. The catalytic performance of Pt–Ni–TiO₂/C catalyst is evaluated and compared to those of homemade Pt–Ni/C and commercial Pt–Ru/C catalyst by CV, chronoamperometry and CO-stripping voltammetry. A combination of analytical techniques including XRD, TEM, XPS and EDX are employed to characterize these catalysts. The aim of this project is to investigate the effects of introducing TiO₂NTs into Pt–Ni and to discuss the feasibility of a low-cost DEFC anode catalyst.

2. EXPERIMENTAL

2.1. Preparation of the Pt–Ni–TiO₂NT/C and Pt–Ni/C catalysts

A detailed description of the preparation of the TiO₂NTs can be found in our previous publication [27]. 5%Pt–10%Ni–10%TiO₂NT/C (wt%, below denoted as Pt–Ni–TiO₂NT/C) catalysts are prepared via a continuous microwave irradiation method. Appropriate amounts of chloroplatinic acid (5 wt% Pt) and nickelous acetate (10 wt% Ni) are added into an ethylene glycol solvent containing TiO₂NTs (5.9 wt% Ti) and carbon Vulcan XC 72R (Cabot Corp.). The pH of the solution is adjusted to above 9 with the use of 0.5 M NaOH. The solution is homogenized via sonication and irradiated for 60s under 700W in a continuous microwave reactor. The filtered products are thoroughly washed with distilled water and dry in vacuum oven overnight. A 5%Pt–10%Ni/C catalyst without TiO₂NTs (named Pt–Ni/C) is also synthesized following the same procedure. A commercial 20%Pt–10%Ru/C (named Pt–Ru/C) was employed for comparison.

2.2. Characterization of the Pt–Ni–TiO₂NT/C and Pt–Ni/C catalysts

Elemental analysis is carried out using an ICP-OES spectrometer (Varian). EDX measurements are done on a Toshiba S-520 SEM.

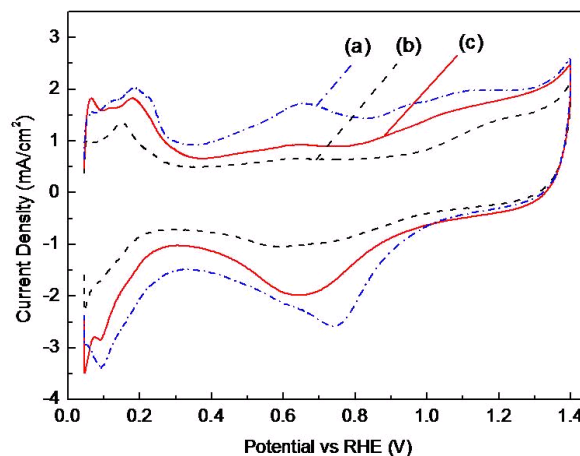


Figure 1. CV of Pt–Ru/C (a), Pt–Ni/C (b), and Pt–Ni–TiO₂NT/C (c) catalysts in 0.5M H₂SO₄ solution at room temperature, with a scan rate of 50mV/s

XRD data is obtained from a Rigakuminiflex diffractometer with Cu K_α radiation ($\lambda = 0.1541$ nm). The morphology and the distributions of the Pt nanoparticle and TiO₂NTs are examined by TEM in a JEOL JEM-2100F (Instrumental Analysis Center of Shanghai Jiao Tong University) at an accelerated voltage of 200 kV. XPS spectra are acquired on a PHI 5000C ESCA spectrometer. X-ray anode used is Al and the base pressure is $\sim 10^{-8}$ Pa. The binding energies are calibrated with reference to the C 1s XPS (284.7 eV) of Vulcan XC-72. XPSPeak 4.1 software is used for the deconvolution of the XPS spectra.

2.3. Electrochemical Measurements

Electrochemical measurements are carried out on a CHI 604 electrochemical workstation (CH Instrument). A conventional three-electrode cell is used with a glassy carbon (GC, 3 mm diameter) as the working electrode. A Pt wire and a saturated calomel electrode (SCE) are employed as the counter and the reference electrode, respectively.

5 mg of catalyst are dispersed into 1 ml of doubly-distilled water and then mixed with 50 μ l Nafion solution, followed by 30 min of ultrasonic treatment. Around 6 μ l of the resulting catalyst solution is then pipetted onto the GC electrode and dried. CV tests are carried out in de-oxygenated electrolytes after bubbling nitrogen for 30 min. Voltammograms are recorded after reproducible curves are obtained. C₂H₅OH is then introduced to the solution. All electrode potentials reported here are against the reversible hydrogen electrode (RHE).

3. RESULTS AND DISCUSSION

3.1. Electrochemical Performances

Figure 1 shows the CVs of the commercial Pt–Ru/C, homemade Pt–Ni/C and Pt–Ni–TiO₂NT/C catalysts in 0.5 M H₂SO₄ solution at room temperature and a scan rate of 50 mV/s. All the curves clearly show the hydrogen adsorption-desorption region (between 0.04–0.36 V). The charge exchanged during the adsorption (Q_a) and desorption (Q_d) of H₂ on Pt sites is evaluated and the electrochemi-

cal active surface (EAS) area was calculated by means of the equation (1) and (2) [28].

$$Q_H = (Q_a + Q_d) / 2 \quad (1)$$

$$EAS = Q_H / ([Pt] \times 0.21) \quad (2)$$

Table 1 shows the EAS of above three catalysts calculated from Fig. 1. The EAS area decreases as follows: Pt-Ni-TiO₂NT/C > Pt-Ni/C > Pt-Ru/C. This result indicates that the Pt-Ni-TiO₂NT/C catalyst has the largest EAS although the Pt content of Pt-Ni-TiO₂NT/C catalyst is only one quarter of Pt-Ru/C catalyst.

Figure 2 shows the CV of the above three catalysts in N₂ saturated 0.5 M H₂SO₄ containing 0.5 M C₂H₅OH solutions. The peak potential for ethanol oxidation in the positive scan direction is significantly lower in the case of Pt-Ni-TiO₂NT/C catalyst (at 0.892 V vs. RHE), versus those of Pt-Ni/C and Pt-Ru/C catalysts (both at around 0.925 V vs. RHE). Similarly, the onset potential of the EOR is lower with the Pt-Ni-TiO₂NT/C catalyst than that of either Pt-Ni/C or Pt-Ru/C catalysts. This may be related to a surface modification where the addition of TiO₂NTs provides more OH radical species, oxidizing the CO-like intermediates formed during the oxidation reaction, at lower potentials [29]. Therefore, a lower onset potential resulted for the Pt-Ni-TiO₂NT/C catalyst. Furthermore, the current density of the Pt-Ni-TiO₂NT/C catalyst (15.75 mA/cm²) is higher by ca. 50% than that of the Pt-Ni/C catalyst (10.10 mA/cm²). This clearly indicates that the addition of TiO₂ nanotubes can greatly improve the catalytic activity for the EOR. The current density of the Pt-Ru/C catalyst is 19.87 mA/cm², which is higher than those of both Pt-Ni/C and Pt-Ni-TiO₂NT/C catalysts. However, the Pt content of the former is almost 4 times higher than the content in the two latter cases. Table 2 shows the mass specific current densities (called MSCD, mA/mg Pt) of above three catalysts based on the results from Fig. 2. Thus, the MSCD of the Pt-Ni-TiO₂NT/C catalyst is 696.0 mA/mg Pt, which is about 3 times higher than those of the Pt-Ru/C catalyst (211.0 mA/mg Pt) and the Pt-Ni/C catalyst (215.4 mA/mg Pt) (see Table 2). It seems that

Table 1. Table 1 The EAS of Pt-Ru/C, Pt-Ni/C and Pt-Ni-TiO₂NT/C catalysts : derived from CV measurements as shown in Figure 1

	[Pt] mg/cm ²	Q _a mC/cm ²	Q _d mC/cm ²	Q _H mC/cm ²	EAS m ² /g cat.
Pt-Ru/C	0.0849	4.50	3.64	4.07	22.8±2.4
Pt-Ni/C	0.0212	2.32	2.29	2.31	51.7±0.4
Pt-Ni-TiO ₂ NT/C	0.0212	4.16	4.3	4.23	94.9±1.6

Table 2 Mass specific current densities of Pt-Ru/C, Pt-Ni/C and Pt-Ni-TiO₂NT/C catalysts derived from the CV curves in Figure 2

	C ₂ H ₅ OH oxidation			Oxidation of intermediates		
	Potential	Current density	Current density / amount of Pt	Potential	Current density	Current density / amount of Pt
	V	mA/cm ²	mA/mg Pt	V	mA/cm ²	mA/mg Pt
Pt-Ru/C	0.926	19.87	234.1	0.662	17.91	211.0
Pt-Ni/C	0.929	10.10	476.0	0.621	4.57	215.4
Pt-Ni-TiO ₂ NT/C	0.892	15.75	742.2	0.621	14.77	696.0

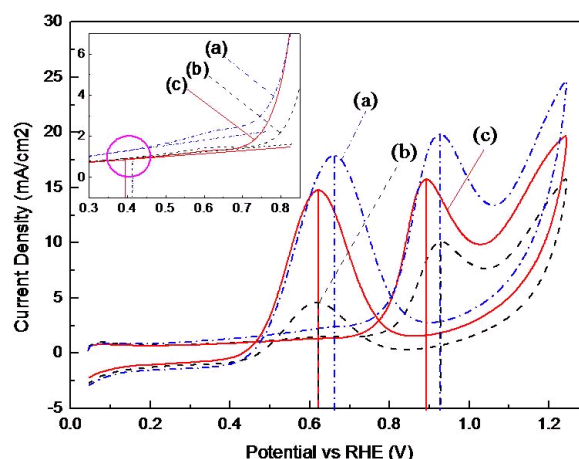


Figure 2. CV of Pt-Ru/C (a), Pt-Ni/C (b), and Pt-Ni-TiO₂NT/C (c) catalysts in 0.5M H₂SO₄ + 0.5M C₂H₅OH solution at room temperature with a scan rate of 50mV/s

TiO₂NT should improve the utilization ratio of Platinum as a promoter in Pt-Ni/C catalyst.

The peaks at more negative potentials in Fig. 2 (negative-going scan) correspond to the oxidation of the reaction intermediates generated from the decomposition of ethanol. The peak current density of the Pt-Ni-TiO₂NT/C catalysts emerges at 0.621 V, which is similar to that of Pt-Ni/C catalyst (0.621 V) and lower than that of Pt-Ru/C catalyst (0.662 V). However, the peak current density of the Pt-Ni-TiO₂NT/C catalyst (14.77 mA/cm²) is significantly higher than that of Pt-Ni/C catalyst (4.57 mA/cm²). This suggests that the addition of TiO₂NTs can facilitate oxidative removal of the reaction intermediates and offer a better catalytic resistance against poisoning by such species. Hence, homemade Pt-Ni-TiO₂NT/C catalysts exhibit better catalytic behavior in the EOR as well as improved catalytic stability.

The CO stripping test is another method that can directly reflect the tolerance of the anode catalysts to CO-like poisoning species. Figure 3 shows the CO stripping curves of the above three catalysts in N₂ saturated 0.5 M H₂SO₄ containing 0.5 M of C₂H₅OH. The potential at peak current density for Pt-Ni-TiO₂NT/C catalyst is earlier than those of the Pt-Ru/C catalyst and the Pt-Ni/C catalyst, similar to the results from the CVs (Fig.2). This suggests that the Pt-Ni-TiO₂NT/C catalyst can oxidize CO more quickly and easily at lower potentials than others. Such fast CO oxidation is helpful to release Pt active sites to further oxidize ethanol molecules. More-

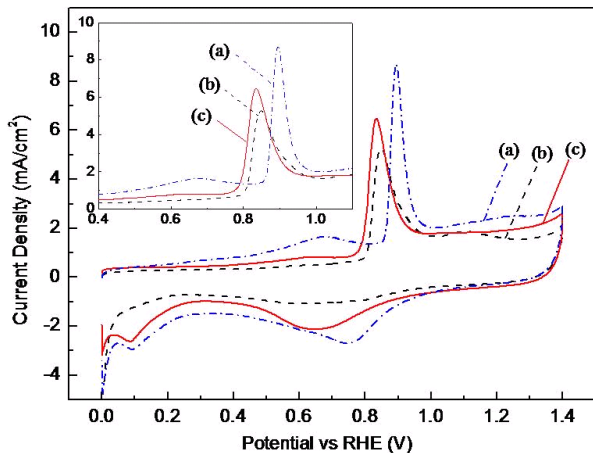


Figure 3. CO-stripping voltammograms of Pt-Ru/C (a), Pt-Ni/C (b), and Pt-Ni-TiO₂NT/C (c) catalysts in 0.5M H₂SO₄ solution at room temperature with a scan rate of 50mV/s

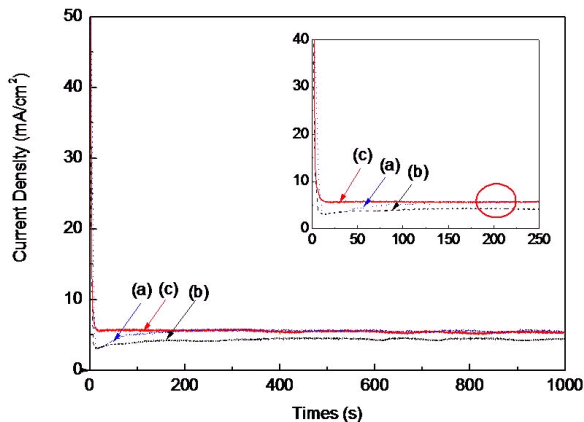


Figure 4. Chronoamperometric curves of Pt-Ru/C (a), Pt-Ni/C (b), and Pt-Ni-TiO₂NT/C (c) catalysts in 0.5M H₂SO₄ + 0.5M C₂H₅OH solution at room temperature

over, the current density of the Pt-Ni-TiO₂NT/C catalyst (6.47mA/cm²) is higher than that of the Pt-Ni/C catalysts (5.27mA/cm²), showing an improvement in catalytic activity for CO removal when TiO₂NTs were introduced into the catalyst surface. In fact, similar results have also been reported by Hogarth et al., where they found that the catalytic activity of Pt electrodes supported on TiO_{2-x} is comparable to that of the best commercial alloy catalyst for alcohol oxidation [30].

A short durability test (Fig. 4) of above three catalysts was performed, corresponding to the peak current density for the EOR in N₂ saturated 0.5 M H₂SO₄ containing 0.5 M C₂H₅OH at room temperature. In all cases, the initial high currents at short times mainly originate from a double-layer charging. Pt-Ni-TiO₂NT/C catalyst is found to decay to steady current density 5.7 mA/cm² within 14s while Pt-Ni/C catalyst decays to steady current density 3.4 mA/cm² till 25 s. The most interesting finding is that the current density of

Table 3 Elemental contents acquired from ICP and EDX for Pt-Ni-TiO₂NT/C catalyst.

Measurement method	Pt (wt%)	Ni (wt%)	Ti (wt%)
ICP	4.24±0.81%	6.78±1.40%	3.37±0.69%
EDX	17.50%	8.05%	2.54%
Theoretical content	5%	10%	5.90%

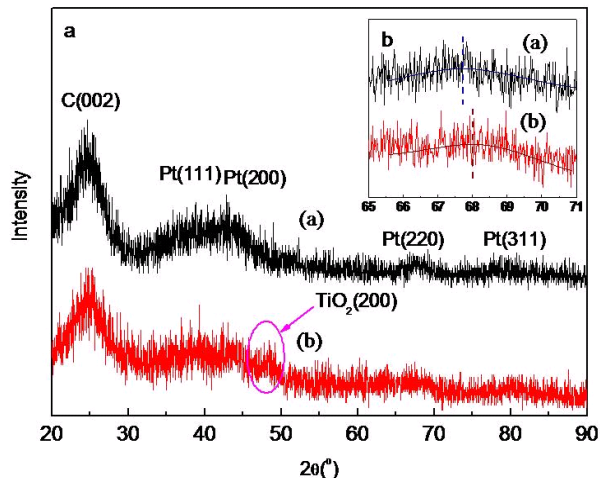


Figure 5. XRD data acquired for Pt-Ni/C (a) and Pt-Ni-TiO₂NT/C (b) catalysts

Pt-Ru/C catalyst drops to 3.1 mA/cm² at 15s then climbs slowly to 5.7 mA/cm² around 200s. However, the current density of the Pt-Ni-TiO₂NT/C catalyst clearly stabilized to higher values than that of the Pt-Ni/C catalyst and to similar values with Pt-Ru/C catalyst.

3.2. Catalyst Characterization

Table 3 shows the elemental composition of the Pt-Ni-TiO₂NT/C catalyst measured by ICP and EDX together with the initial theoretical quantity. The Pt content by ICP is 4.24% which is similar to the theoretical value (5%), but the content of both Ni and Ti deviate obviously from the theoretical values. EDX shows the Pt content to be 17.50%, which is three times greater than the theoretical value. It can be concluded that the Pt active species is well dispersed throughout the surface region, which induces the higher EAS of Pt-Ni-TiO₂NT/C catalyst (Table 1).

Figure 5 shows the XRD data acquired for the Pt-Ni/C and Pt-Ni-TiO₂NT/C catalysts. The common feature at 24.6 ° can be ascribed to the (002) reflection of graphite carbon. Both Pt-Ni/C and Pt-Ni-TiO₂NT/C catalysts show weak and broad (111), (200), and (220) peaks. The inset of Fig. 5 shows that the Pt-Ni-TiO₂NT/C catalyst has a little shift of Pt(220) to higher 2θ than Pt-Ni/C catalyst. The lattice constants for Pt, calculated based on the (220) peak positions [31] are 0.3909 and 0.3897 nm for Pt-Ni/C and Pt-Ni-TiO₂NT/C catalysts respectively. The much smaller lattice constant seen after the introduction of TiO₂NTs indicates that the Pt-Ni alloy should be improved to result in a shrinking of Pt-Pt distances. As most Ni species might exist in oxide forms, no Ni species peak is detected. One small but reproducible peak can be seen at approxi-

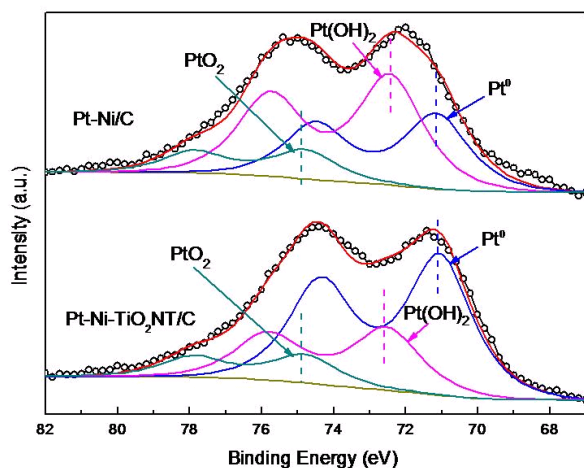


Figure 6. Pt 4f XPS spectra acquired for Pt-Ni-TiO₂NT/C and Pt-Ni/C catalysts

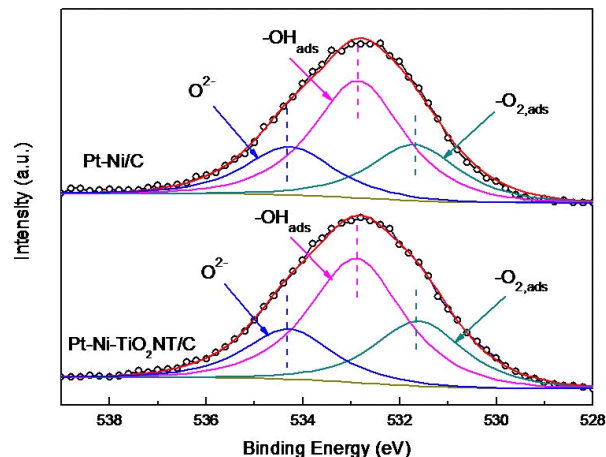


Figure 8. O 1s XPS spectra acquired for Pt-Ni-TiO₂NT/C and Pt-Ni/C catalysts

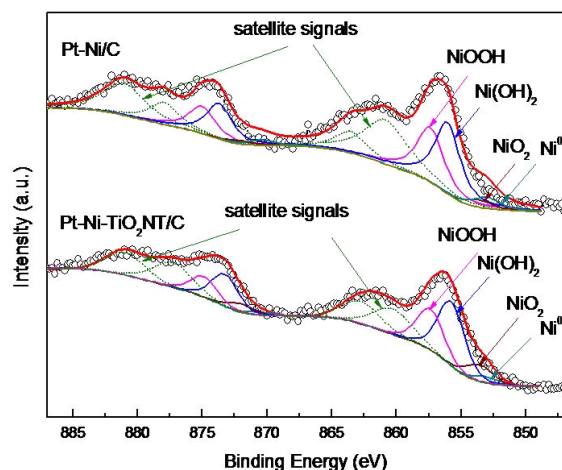


Figure 7. Ni 2p XPS spectra acquired for Pt-Ni-TiO₂NT/C and Pt-Ni/C catalysts

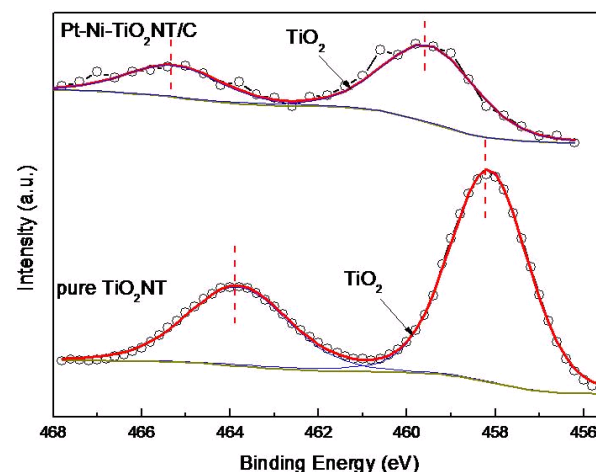


Figure 9. Ti 2p XPS spectra acquired for Pt-Ni-TiO₂NT/C catalyst and pure TiO₂NTs material

mately 48° in the XRD patterns of the Pt-Ni-TiO₂NT/C catalyst. This peak can belong to the (200) diffraction peak of anatase TiO₂. No other common peaks of anatase TiO₂ are detected.

XPS can provide electronic information of the catalytic species and of their interactions. This paper employs XPS Peak 4.1 software for the deconvolution of the XPS spectra [32]. Figure 6 shows the Pt 4f XPS spectra acquired for Pt-Ni/C and Pt-Ni-TiO₂NT/C catalysts. Both spectra of Pt 4f are fitted by taking into account the presence of three platinum oxidation states [33]. It is obvious that the addition of TiO₂NTs dramatically increases the amount of Pt metallic species at the expense of Pt(OH)₂ species. This indicates that some of the hydroxide species on Pt may migrate and combine with TiO₂ species. Thus more Pt elements are either kept in metallic form or formed an alloy with Ni. The increase of active Pt⁰ sites is necessary for the enhancement seen in electrochemical activities.

Figure 7 shows the Ni 2p XPS region acquired for the above catalysts. In accordance with previous reports [15, 34, 35], the XPS

peaks associated with Ni, NiO, Ni(OH)₂, and NiOOH species are located at 852.98, 853.51, 856.04, and 857.38 eV, respectively. There is close to 10 % of metallic Ni species in both cases, less than what is found in Pt-Ni/C catalyst reduced by NaBH₄ [15]. This can be due to fact that, in our case, NaOH is introduced to adjust pH and Ni(OH)₂ was formed during that process. The addition of TiO₂NTs slightly increases the amount of NiO at the expense of Ni(OH)₂ and NiOOH species. This might occur because some of the hydroxide groups are incorporated onto the TiO₂NT surfaces.

Figure 8 shows the O 1s XPS region of these two catalysts. The three O 1s XPS peaks correspond to the oxygen lattice, adsorbed hydroxide group and adsorbed molecular oxygen in these catalysts [15]. Notably, the amount of hydroxide groups in Pt-Ni-TiO₂NT/C catalyst is 20 % higher than that in Pt-Ni/C catalyst. This is in good accordance with the Pt 4f discussed above. In conclusion, the TiO₂NTs can be an excellent source of oxygen species, the presence of which leads to a faster oxidation of the reaction intermedi-

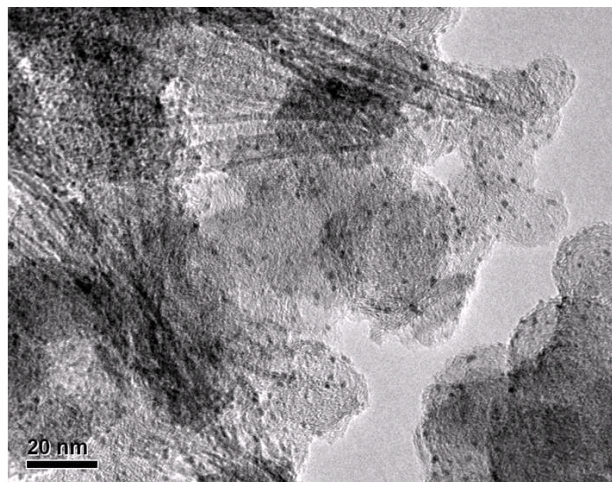


Figure 10. TEM image of Pt-Ni-TiO₂NT/C catalyst

ates and to a slower deactivation process of the catalysts.

In order to study the electron environment of Ti element in TiO₂NTs promoted Pt-Ni/C catalyst, Ti 2p XPS regions of Pt-Ni-TiO₂NT/C catalyst and pure TiO₂NT material are illuminated in Figure 9. Both of them contain pure TiO₂ species, but the Ti 2p peak of the Pt-Ni-TiO₂NT/C catalyst shifts to higher electron binding energy compared with the latter. The 1.4 eV shift tells that the Ti in Pt-Ni-TiO₂NT/C catalyst offer some electron clouds to others. In view of more amount of metallic Pt which implies that Pt species tend getting electrons in this catalyst from fig. 6, it can be concluded that Ti provides some electron clouds to Pt.

Finally, Figure 10 shows the TEM image of the Pt-Ni-TiO₂NT/C catalyst. The results suggest that Pt, Ni or PtNi and TiO₂ nanotubes are highly dispersed on the carbon support. Some of the Pt or Ni or PtNi nanoparticles are surprisingly found on the surface of the TiO₂ nanotubes. The interaction among Pt, Ni, TiO₂NTs and Vulcan XC-72 carbon can explain the good catalytic activity of the Pt-Ni-TiO₂NT/C catalyst on EOR. The formation of carbon deposits during the EOR can be inhibited by the presence of more hydroxide groups provided by TiO₂NTs, thus significantly reducing the poisoning of Pt active sites [21].

4. CONCLUSIONS

The introduction of TiO₂NTs into the Pt-Ni/C catalyst can significantly improve the performance and the time-stability of the Pt-Ni-TiO₂/C catalysts on the EOR. The TiO₂NTs promoted low-Pt content (5 wt%) carbon-supported Pt-Ni-TiO₂NT/C catalyst has a larger EAS than commercial Pt-Ru/C catalyst in addition to a lower onset potential for the EOR, corresponding to a faster current rise. The EOR current density generated by Pt-Ni-TiO₂NT/C catalyst is roughly 75% of that by Pt-Ru/C catalyst, however, the platinum content of the former is only one quarter of the latter. Our research shows that TiO₂NTs doped Pt-Ni/C catalysts with low-Pt content have exceptional potential as a new type of anode catalysts for ethanol oxidation. In conclusion, the presence of TiO₂ nanotubes modifies the electronic structure of Pt in terms of creating more metallic sites. More hydroxide groups are also generated, which participate in the oxidative removal of the reaction intermediates

thus increasing catalyst efficacy Pt catalysts by minimizing site-blocking.

5. ACKNOWLEDGMENTS

The authors are grateful for the financial support of this work by the National 863 Program (2007AA05Z145), National Science Foundation of China (20776085), Science and Technology Commission of Shanghai Municipality (07JC14024, 09XD1402400) and the support from Instrumental Analysis Centre of Shanghai Jiao Tong University. The authors also wish to acknowledge the National Council for Science and Technology (Conacyt-Mexico) for financial support through the Bilateral Collaboration program.

REFERENCES

- [1] W. Zhou, Z. Zhou, S. Song, W. Li, G. Sun, P. Tsiakaras and Q. Xin, *Appl. Catal. B: Env.*, 46, 273 (2003).
- [2] E. Antolini, *J. Power Sources*, 170, 1 (2007).
- [3] S. Song, P. Tsiakaras, *Appl. Catal. B: Env.*, 63, 187 (2006).
- [4] E. Peled, T. Duvdevani, A. Aharon, *Electrochem. Solid-State Lett.*, 4, A38 (2001).
- [5] C. Roth, A.J. Papworth, I. Hussain, R.J. Nichols, D.J. Schiffrin, *J. Electroanal. Chem.*, 581, 79 (2005).
- [6] S. Lj. Gojkovic, T.R. Vidakovic, D.R. Durovic, *Electrochim. Acta*, 48, 3607 (2003).
- [7] C. Lu, C. Rice, R.I. Masel, P.K. Babu, P. Waszczuk, H.S. Kim, E. Oldfield, A. Wieckowski, *J. Phys. Chem. B*, 106, 9581 (2002).
- [8] P. Waszczuk, G.-Q. Lu, A. Wieckowski, C. Lu, C. Rice, R.I. Masel, *Electrochim. Acta*, 47, 3637 (2002).
- [9] T. Frelink, W. Visscher, J.A.R. Van Veen, *Surf. Sci.*, 335, 353 (1995).
- [10] S.A. Lee, K.W. Park, J.H. Choi, B.K. Kwon, Y.E. Sung, *J. Electrochem. Soc.*, 149, A1299 (2002).
- [11] J. Kua, W.A. Goddard III, *J. Am. Chem. Soc.*, 121, 10928 (1999).
- [12] F.J. Rodriguez-Nieto, T.Y. Morante-Catacora, C.R. Cabrera, *J. Electroanal. Chem.*, 571, 15 (2004).
- [13] L.H. Jiang, G.Q. Sun, Z.H. Zhou, W.J. Zhou, Q. Xin, *Catal. Today*, 93–95, 665 (2004).
- [14] U.A. Paulus, A. Wokaun, G.G. Scherer, T.J. Schmidt, V. Stamenkovic, V. Radmilovic, N.M. Markovic, P.N. Ross, *J. Phys. Chem. B*, 106, 4181 (2002).
- [15] K.W. Park, J.H. Choi, B.K. Kwon, S.A. Lee, Y.E. Sung, H.Y. Ha, S.A. Hong, H.S. Kim, A. Wieckowski, *J. Phys. Chem. B*, 106, 1869 (2002).
- [16] T.C. Deivaraj, W.X. Chen, J.Y. Lee, *J. Mater. Chem.*, 13, 2555 (2003).
- [17] Z.B. Wang, G. P. Yin, J. Zhang, Y.C. Sun, P.F. Shi, *J. Power Sources*, 160, 37 (2006).
- [18] E. Ribadeneira, B.A. Hoyos, *J. Power Sources*, 180, 238 (2008).
- [19] E. Spinacé, M. Linardi, A. Oliveira, *Electrochem. Commun.*, 7, 365 (2005).
- [20] D.B. Chu, X.F. Zhou, C.J. Lin, J.G. Tan, *Direct Electrochemi-*

- cal Synthesis of Metal Alkoxides, Chem. J. Chinese U., 2000, 21 (1): 133~135.
- [21]H.Q. Song, X.P. Qiu, F.S. Li, W.T. Zhu, L.Q. Chen, Electrochem. Commun., 9, 1416 (2007).
- [22]B.E. Hayden, D.V. Malevich, D. Pletcher, Electrochem. Commun., 3, 395 (2001).
- [23]F. Hu, F. Ding, S. Song, P.K. Shen, J. Power Sources, 163, 415 (2006).
- [24]J.M. Macak, P.J. Barczuk, H. Tsuchiya, M.Z. Nowakowska, A. Ghicov, M. Chojak, S. Bauer, S. Virtanen, P.J. Kulesza, P. Schmuki, Electrochem. Commun., 7, 1417 (2005).
- [25]X. Wu, Q.Z. Jiang, Z. Ma, L.Q. Hu, Chinese J. Power Sources, 31, 713 (2007).
- [26]Q.Z. Jiang, X. Wu, M. Shen, Z. Ma, X.Y. Zhu, Catal. Lett., 124, 434 (2008).
- [27]X. Wu, Q.Z. Jiang, Z.F. Ma, M. Fu, W.F. Shangguan, Solid State Commun., 136, 513 (2005).
- [28]A. Pozio, M. De Francesco, A. Cemmi, F. Cardellini, L. Giorgi, J. Power Sources, 105, 13 (2002).
- [29]J. Luo, P.N. Njoki, Y. Lin, D. Mott, L. Wang, C.J. Zhong, Langmuir, 22, 2892 (2006).
- [30]M.P. Hogarth, G.A. Hards, Plat Met Rev, 40, 150 (1996).
- [31]V. Radmilović, H.A. Gasteiger, P.N. Ross Jr, Journal of Catalysis, 154, 98 (1995).
- [32]<<http://www.phy.cuhk.edu.hk/~surface/XPSPEAK>>.
- [33]A. Seo, J.S. Lee, K. Han, H. Kim, Electrochem. Acta., 52, 1603 (2006).
- [34]Y. Zhao, Y.F. En, L.Z. Fan, Y.F. Qiu, S.H. Yang, Electrochem. Acta., 52, 5873 (2007).
- [35]M.A. Garcia-Contreras, S.M. Fernandez-Valverde, J.R. Vargas-Garcia, M.A. Cortes-Jacome, J.A. Toledo-Antonio, C. Angeles-Chavez, Int. J. Hydrogen Energy, 33, 6672 (2008).